We are IntechOpen, the world's leading publisher of Open Access books Built by scientists, for scientists

4,800
Open access books available

122,000
International authors and editors

135M
Downloads

Our authors are among the

154
Countries delivered to

TOP 1%
most cited scientists

12.2%
Contributors from top 500 universities

CLARIVATE ANALYTICS BOOK CITATION INDEX INDEXED

WEB OF SCIENCE™

Selection of our books indexed in the Book Citation Index in Web of Science™ Core Collection (BKCI)

Interested in publishing with us?
Contact book.department@intechopen.com

Numbers displayed above are based on latest data collected.
For more information visit www.intechopen.com

27

Dynamic Visual Servoing with an Uncalibrated Eye-in-hand Camera[1]

Hesheng Wang and Yun-Hui Liu
The Chinese University of Hong Kong
China

1. Introduction

Visual servoing is an approach to control motion of a robot manipulator using visual feedback signals from a vision system. Though the first systems date back to the late 1970s and early 1980s, it is not until the middle 1990s that there is a sharp increase in publications and working systems, due to the availability of fast and affordable vision processing systems (Hutchinson et al, 1996).
There are many different ways of classifying the reported results: based on number of cameras used, generated motion command (2D, 3D), camera configuration, scene interpretation, underlying vision algorithms. We will touch upon these issues briefly in the following sections.

1.1 Image-based and Position-based Visual Servoing

Visual servo robot control overcomes the difficulties of uncertain models and unknown environments. Existing methods can be classified into two basic schemes, namely position-based visual servo control (Fig. 1) and image-based visual servo control (Fig. 2). In both classes of methods, object feature points are mapped onto the camera image plane, and measurements of these points are used for robot control. A combination of the two schemes is called hybrid visual servoing.
A position-based approach first uses an algorithm to estimate the 3-D position and orientation of the robot manipulator or the feature points from the images and then feeds the estimated position/orientation back to the robot controller. The main advantage of position-based visual servoing is that it controls the camera trajectory in the Cartesian space, which allows it to easily combine the visual positioning task with obstacles avoidance and singularities avoidance. Position-based methods for visual servoing seem to be the most generic approach to the problems, as they support arbitrary relative position with respect to the object. The major disadvantage of position-based methods is that the 3D positions of the feature points must be estimated. In position-based visual servoing, feedback is computed using estimated quantities that are a function of the system calibration parameters. Hence, in some situations, position-based control can become extremely sensitive to calibration error. Since 3-D position/orientation estimation from images is subject to big noises,

[1] This work is partially supported by Hong Kong RGC under the grant 414406 and 414707, and the NSFC under the projects 60334010 and 60475029. Y.-H. Liu is also with Joint Center for Intelligent Sensing and Systems, National University of Defense Technology, Hunan, China.

position-based methods are weak to disturbances and measurement noises. Therefore, the position-based visual servoing is usually not adopted for servoing tasks.

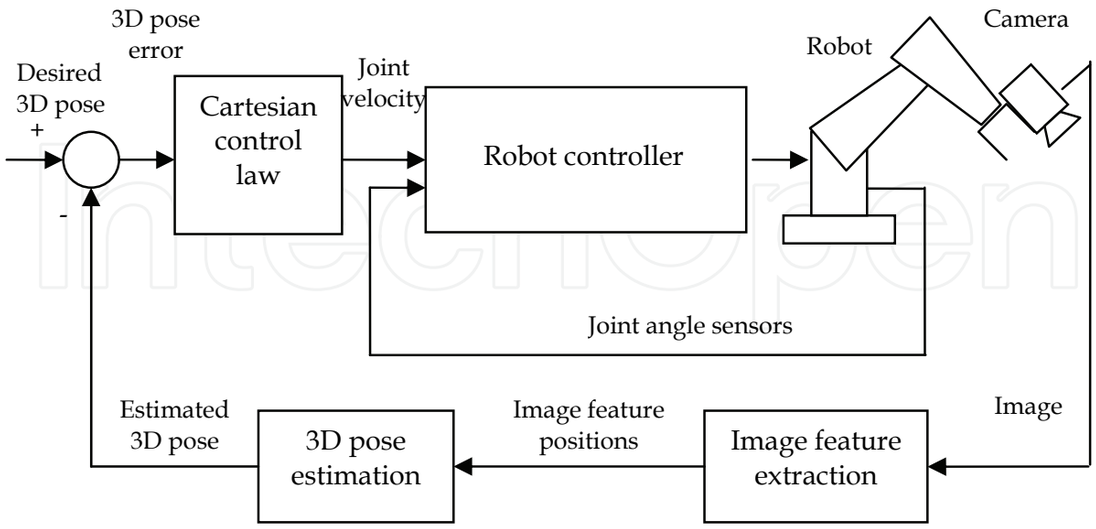

Figure 1. Position-based visual servoing

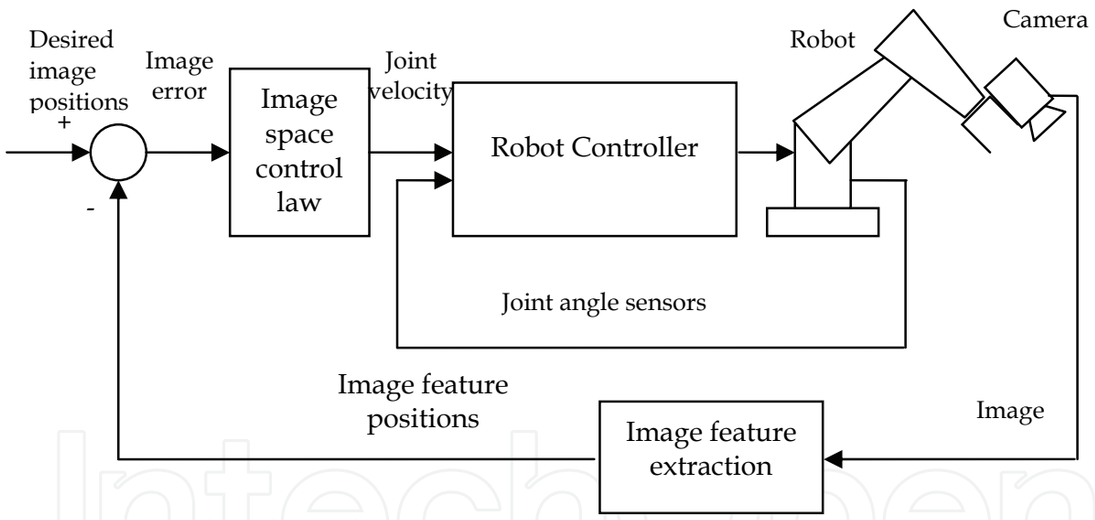

Figure 2. Image-based visual servoing

An image-based approach selects a set of feature points on the robot or the target object and directly employs their projection signals on the image plane of the camera in robot control. The general approach used in the image-based visual control methods is to control the robot motion in order to move the image plane features to desired positions. This usually involves the calculation of an image Jacobian or a composite Jacobian, the product of the image and robot Jacobian. A composite Jacobian relates differential changes in joint angles to differential changes in image features. The image-based control has the input command described directly in the feature space; it is then easy to generate the input trajectory. Since the feedback signals are projection errors on the image plane, image-based controllers are considered more robust to disturbances than position-based methods. Coarse calibration only affects the rate of convergence of the control law in the sense that a longer time is needed to reach the desired

position. One disadvantage of image-based methods compared to position-based methods is the presence of singularities in the feature mapping function, which reflect themselves as unstable points in the inverse Jacobian control law. The estimation of the image Jacobian requires knowledge of the camera intrinsic and extrinsic parameters. Extrinsic parameters also represent a rigid mapping between the scene or some reference frame and the camera frame. If one camera is used during the servoing process, the depth information needed to update the image Jacobian is lost. Therefore, many of the existing systems usually rely on a constant Jacobian that is computed for the desired camera/end–effector pose. This is one of the drawbacks of this approach, since the convergence is ensured only around the desired position. This problem may be solved by adaptive estimation of the depth.

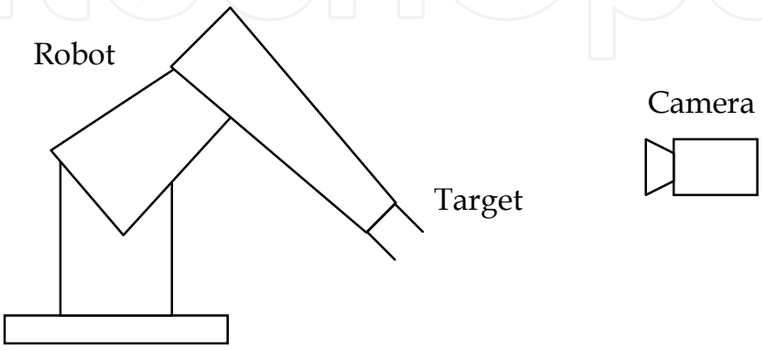

Figure 3. Fixed camera configuration

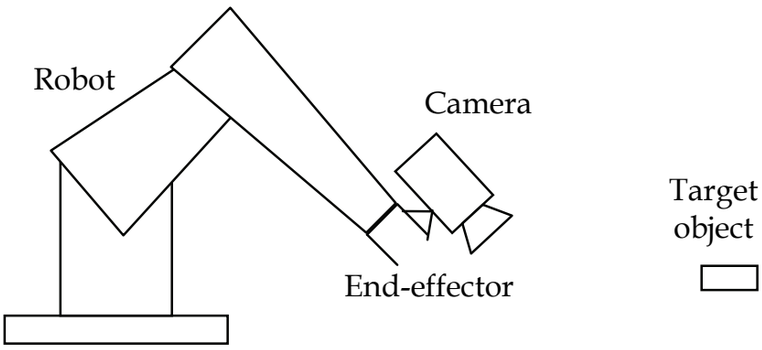

Figure 4. Eye-in-hand camera configuration

1.2 Fixed Camera and Eye-in-hand Configurations

There are two possible configurations, namely fixed camera (eye-to-hand) configuration (Fig. 3) and eye-in-hand configuration (Fig. 4), to set up a vision system for visual servo control of robot manipulators.

In a fixed camera setup, targets are mounted on a robot end-effector and the camera is fixed at a position near the manipulator. In this case, the camera does not move with the robot manipulator and its objective is to monitor motion of the robot.

In an eye-in-hand setup, the camera is mounted at the end-effector of the robot manipulator so that it moves with the manipulator. The camera is to measure information of objects in the surrounding environment. The objective of this approach is to move the manipulator in such a way that the projection of either a moving or a static object be always at a desired location in the image captured by the camera

While each configuration has its own advantages and drawbacks, they both can be found in real applications. Eye-in-hand systems can be widely found in research laboratories and are being used in tele-operated inspection systems in hazardous environments such as nuclear factories. Fixed camera setups are used in vision-based pick-and-place at manufacturing lines, robots assisted by networked cameras, etc.

1.3 Kinematics-based and Dynamic Visual Servoing

Existing methods can also be classified into kinematics-based (Fig. 5) and dynamic methods (Fig. 6). Kinematics-based methods do not consider the nonlinear dynamics of the robot manipulator and design the controller based on the kinematics only. Kinematics-based methods decouple the designs of motion controller of manipulators and the visual controller under the assumption that the manipulator can perfectly perform the position or velocity control required in visual servoing. They change visual servoing into a problem of designing the velocity or position of the end-effector of the robot using the visual feedback signals. It is well known that the nonlinear robot forces have significant impact on robot motion, especially when the robot manipulator moves at high speed. Neglecting them not only decays the control accuracy but also results in instability. In a rigorous sense, the stability is not guaranteed for all kinematics-based controllers. Kinematics-based controllers are suitable for slow robot motion only.

Dynamic methods design the joint input directly, instead of the velocity of the end-effector, using the visual feedback and include the nonlinear robot dynamics in the control loop. The nonlinear centrifugal and Coriolis forces are compensated for in the control loop. Dynamic controllers guarantee the stability and are suitable for both slow and fast robot motions. Compared to kinematics-based methods, work on dynamic visual servoing is relatively limited, though the importance has been recognized for a long time by many researchers. This is mainly due to the difficulties in incorporating the nonlinear forces in controller design and the existence of the nonlinear scaling factors corresponding to the reciprocal of the depths of the feature points in the perspective projection. Since it is difficult to measure or estimate on-line the depths of the feature points, most dynamic controllers are subject to planar motions of robot manipulators only.

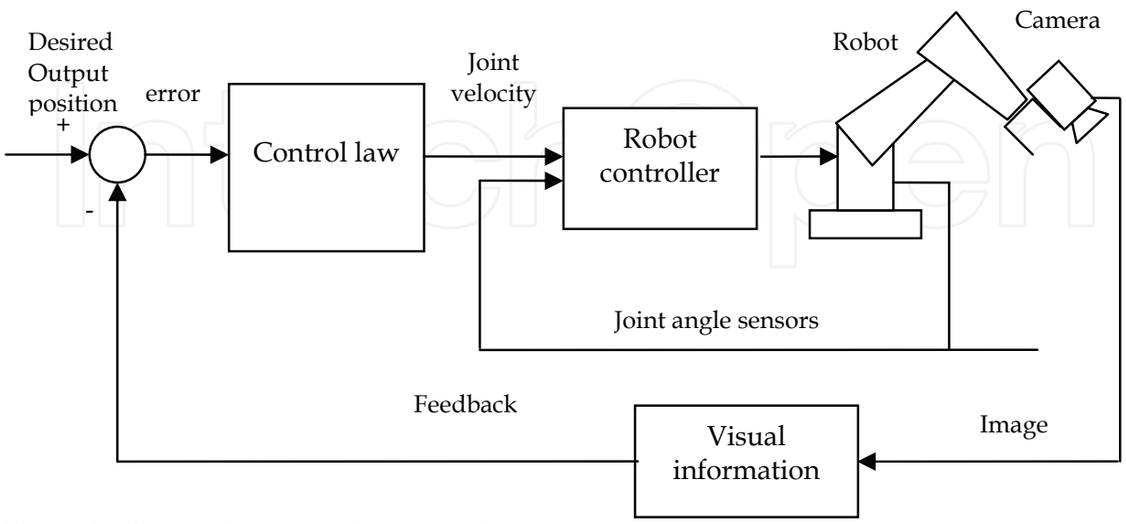

Figure 5. Kinematic-based visual servoing

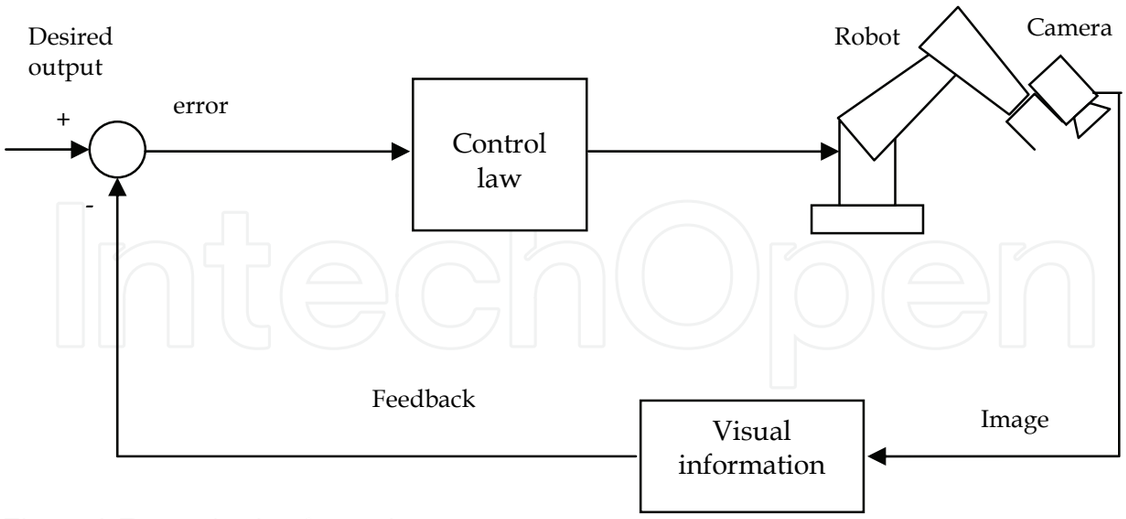

Figure 6. Dynamic visual servoing

1.4 Related Work of Visual Servoing with Uncalibrated Eye-in-hand Camera

Image-based eye-in-hand visual servoing is a problem of controlling the projections of image features to desired positions on the image plane of a camera mounted on a robot manipulator by controlling motion of the manipulator. Compared to a camera fixed in the workspace, an eye-in-hand camera enables the manipulator to view the workspace more flexibly. To implement a visual servo controller, an important step is to calibrate the intrinsic and extrinsic parameters of the camera. It is well known that camera calibration is costly and tedious. A survey of camera self-calibration could be referring to (Hemayed, 2003). To avoid camera calibration, many efforts have been made to uncalibrated visual seroving for which methods can be classified into kinematics-based controllers and dynamic controllers.

In kinematics-based methods, the typical idea for uncalibrated visual servoing is to estimate the image Jaocbian or the depths of the features on-line. (Papanikolopoulos et al, 1995) developed an on-line estimation method to determine the depth information of the feature point. (Malis et al, 1999; 2004) proposed 2-1/2-D visual servoing to deal with uncalibrated camera intrinsic parameters. (Yoshimi & Allan, 1995) proposed an estimator of the image Jacobian for a peg-in-hole alignment task. (Hosoda & Asada, 1994) designed an on-line algorithm to estimate the image Jacobian. (Ruf et al, 1997) proposed a position-based visual servoing by adaptive kinematic prediction. (Pomares et al, 2007) proposed adaptive visual servoing by simultaneous camera calibration. Since the design of visual servo controller does not take the nonlinear robot dynamics into account, the stability of the overall system is not guaranteed even if the visual controller is stable. This is point out by many researchers such as (Bishop & Spong, 1997; Cheah et al, 2003; Deng et al, 2002; Hsu and Aquino, 1999; Kelly et al, 1999; Kim et al, 1995; Dixon, 2007; Shen et al, 2003).

Dynamic methods design the joint input directly, instead of the velocity of the end-effector, using the visual feedback and include the nonlinear robot dynamics in the control loop. (Carelli et al, 2000) proposed an adaptive controller to estimate robot parameters for the eye-in-hand setup. (Kelly et al, 2000) developed an adaptive controller for visual servoing of planar manipulators. The controller developed by (Hashimoto et al, 2002; Nagahama et al 2002) incorporated the nonlinear robot dynamics in controller design and employed a

motion estimator to estimate motion of an object in a plane. In our early work, we proposed a new adaptive controller for uncalibrated visual servoing of 3-D manipulator using a fixed camera (Liu et al, 2005, 2006; Wang & Liu, 2006; Wang et al, 2007). The underlying idea in our controller is the development of the concept of the depth-independent interaction matrix (or image Jacobian) matrix to avoid the depth that appears in the denominator of the perspective projection equation.

1.5 Outline of This Chapter

A brief review of uncalibrated visual servoing is presented in this Chapter. Some prerequisite knowledge including camera parameters, perspective projection models, coordinate transformations, geometry relationship are discussed in detail. Then we focus on one typical problem in visual servoing: visual servoing with uncalibrated eye-in-hand camera.

This paper extends our controller developed before (Liu et al, 2006) to image-based visual servoing of point features using an uncalibrated eye-in-hand camera. In an eye-in-hand setup in addition to the camera parameters, the 3-D coordinates of the features are not known either. Therefore, we need to estimate both the camera parameters and the 3-D coordinates on-line. The basic idea in the controller design is to use the depth-independent interaction (or image Jacobian) matrix so that the depth appearing in the denominator of the perspective projection equation can be avoided. To simultaneously estimate the camera parameters and the unknown 3-D coordinates of the features, we combine the Slotine-Li method with an on-line estimator designed on the basis of the idea of structure from motion in computer vision. The estimator uses the image sequence, captured during motion of the manipulator, to estimate the 3-D structure and the perspective projection matrix on-line by minimizing the Frobenius norm of the estimated projection errors. Based on the nonlinear dynamics of the manipulator, we have proved by the Lyapunov theory that the image errors will be convergent to zero and the unknown camera parameters and 3-D coordinates of the features are convergent to the real values up to a scale. Experiments have been conducted to validate the proposed methods.

This Chapter is organized as follows. Section 2 will review the kinematics and the dynamics. Section 3 will present adaptive image-based visual servoing with unknown target positions. In Section 4, we will discuss adaptive visual servoing with unknown camera parameters and target positions. Section 5 presents the experimental results and Section 6 concludes the major results in this Chapter.

2. Camera and Robot Model

2.1 Problem Definition

Consider an eye-in-hand set-up (Fig. 7), in which a vision system is mounted on the end-effector to monitor a set of target points. Assume that the target points are fixed ones but their coordinates are not known. Suppose that the camera is a pin-hole camera with perspective projection (Fig. 8). Furthermore, we will consider two cases by assuming that the intrinsic parameters of the camera and the extrinsic parameters, i.e. the homogeneous transform matrix between the camera and the end-effector, are known or unknown.

Problem 1: Given desired positions of the target points on the image plane, design a proper joint input for the manipulator such that the projections of the target points on the image

plane is asymptotically convergent to the desired positions. Assuming that only the target 3-D position are unknown.

Problem 2: Given desired positions of the target points on the image plane, design a proper joint input for the manipulator such that the projections of the target points on the image plane is asymptotically convergent to the desired positions. Assuming that both the 3-D coordinates of the target points and the intrinsic and extrinsic parameters of the camera are unknown.

To simplify the discussion, we will assume that the target always remains in the field of view

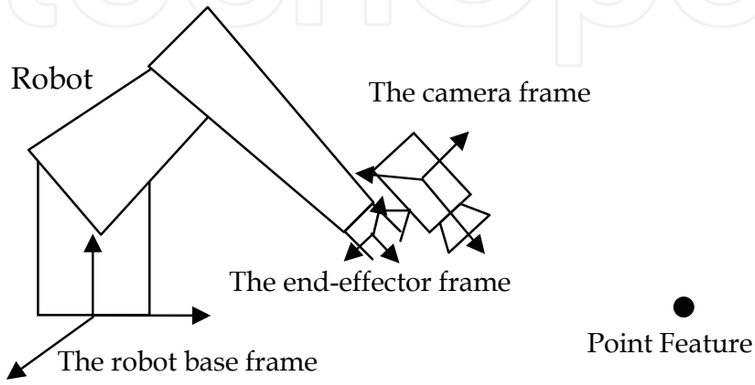

Figure 7. An eye-in-hand setup for visual servoing

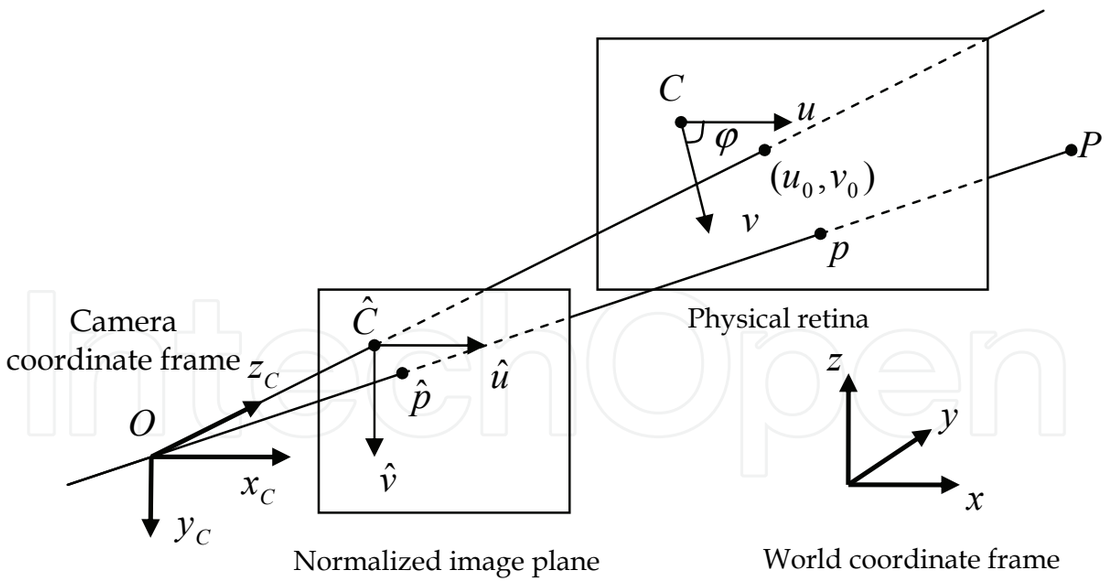

Figure 8. Perspective projection

2.2 Kinematics

In Fig. 7, three coordinate frames, namely the robot base frame, the end-effector frame, and the camera frame, have been set up to represent motion of the manipulator. Denote the joint

angle of the manipulator by $\mathbf{q}(t)$, and the homogenous coordinates of the target w.r.t. the robot base and the camera frames by $\mathbf{x}$ and ${}^{\mathbf{c}}\mathbf{x}$, respectively. Note that the $\mathbf{x}$ is a constant vector for the fixed target point and $\mathbf{x} = \begin{pmatrix} {}^{b}\mathbf{x} & 1 \end{pmatrix}^T$. Denote the homogenous transform matrix of the end-effector with respect to the base frame by $\mathbf{T_e(q)}$, which can be calculated from the kinematics of the manipulator. Denote the homogeneous transformation matrix of the camera frame with respect to the end-effector frame by $\mathbf{T_c}$, which represents the camera extrinsic parameters. From the forward kinematics of the manipulator, we have

$$ {}^{\mathbf{c}}\mathbf{x} = \mathbf{T_c^{-1}} \mathbf{T_e^{-1}}(\mathbf{q})\mathbf{x} \tag{1} $$

where

$$ \mathbf{T}_e^{-1}(t) = \begin{pmatrix} \mathbf{R}(t) & \boldsymbol{\xi}(t) \\ 0 & 1 \end{pmatrix} \tag{2} $$

where $\mathbf{R}(t)$ and $\boldsymbol{\xi}(t)$ are the rotation matrix and the translation vector from robot base frame to end-effector frame.

Let $\mathbf{y} = (u, v, 1)^T$ express the homogenous coordinates of the projection of the target point on the image plane. Under the perspective projection model,

$$ \mathbf{y} = \frac{1}{{}^{c}z} \boldsymbol{\Omega}\, {}^{\mathbf{c}}\mathbf{x} = \frac{1}{{}^{c}z} \boldsymbol{\Omega} \mathbf{T_c^{-1}} \mathbf{T_e^{-1}}(\mathbf{q})\mathbf{x} \tag{3} $$

where $\boldsymbol{\Omega}$ is determined by the camera intrinsic parameters:

$$ \boldsymbol{\Omega} = \begin{pmatrix} \alpha & -\alpha \cot\varphi & u_0 & 0 \\ 0 & \dfrac{\gamma}{\sin\varphi} & v_0 & 0 \\ 0 & 0 & 1 & 0 \end{pmatrix} \tag{4} $$

where α and γ are the scalar factors of the u and v axes of the image plane. φ represents the angle between the two axes. ${}^{c}z$ is the depth of the feature point with respect to the camera frame. Denote by $\mathbf{M}$ the product of $\boldsymbol{\Omega}$ and $\mathbf{T_c^{-1}}$, i.e.,

$$ \mathbf{M} = \begin{pmatrix} \alpha \mathbf{r_1^T} - \alpha \cot\varphi \mathbf{r_2^T} + u_0 \mathbf{r_3^T} & \alpha p_x - \alpha \cot\varphi p_y + u_0 p_z \\ \dfrac{\gamma}{\sin\varphi} \mathbf{r_2^T} + v_0 \mathbf{r_3^T} & \dfrac{\gamma}{\sin\varphi} p_y + v_0 p_z \\ \mathbf{r_3^T} & p_z \end{pmatrix} \tag{5} $$

where $\mathbf{r_i^T}$ denotes the i-th row vector of the rotation matrix of $\mathbf{T_c^{-1}}$, and $(p_x, p_y, p_z)^T$ is its translational vector. The matrix $\mathbf{M}$ is called *perspective projection matrix*, which depends on the intrinsic and extrinsic parameters only. Eq. (3) can be rewritten as

$$ \mathbf{y} = \frac{1}{{}^{c}z} \mathbf{M} \mathbf{T_e^{-1}}(\mathbf{q})\mathbf{x} \tag{6} $$

The depth of the feature point is given by

$$ {}^{c}z = \mathbf{m}_3^{\mathrm{T}}\mathbf{T}_{\mathbf{e}}^{-1}(\mathbf{q})\mathbf{x} \tag{7} $$

Where $\mathbf{m}_3^{\mathrm{T}}$ denotes the third row vector of the perspective projection matrix **M**.

$$ {}^{c}\dot{z} = \underbrace{\frac{\partial(\mathbf{m}_3^{\mathrm{T}}\mathbf{T}_{\mathbf{e}}^{-1}(\mathbf{q})\mathbf{x})}{\partial\mathbf{q}}}_{\mathbf{n}^{\mathrm{T}}(\mathbf{q})}\dot{\mathbf{q}} = \mathbf{n}^{\mathrm{T}}(\mathbf{q})\dot{\mathbf{q}} \tag{8} $$

It is important to note:

Property 1: *A necessary and sufficient condition for matrix* **M** *to be a perspective projection matrix is that it has a full rank.*

By differentiating eq. (6), we obtain the following relation:

$$ \dot{\mathbf{y}} = \frac{1}{{}^{c}z}(\mathbf{M}\dot{\mathbf{T}}_{\mathbf{e}}^{-1}(\mathbf{q}) - \mathbf{y}^{\mathbf{c}}\dot{z}) = \frac{1}{{}^{c}z}\mathbf{A}(\mathbf{q})\dot{\mathbf{q}} \tag{9} $$

where the matrix **A(q)** is a matrix determined by

$$ \mathbf{A}(\mathbf{q}) = \underbrace{\begin{pmatrix} \mathbf{m}_1^{\mathrm{T}} - u\mathbf{m}_3^{\mathrm{T}} \\ \mathbf{m}_2^{\mathrm{T}} - v\mathbf{m}_3^{\mathrm{T}} \\ \mathbf{0} \end{pmatrix}}_{\mathbf{D}} \frac{\partial(\mathbf{T}_{\mathbf{e}}^{-1}(\mathbf{q})\mathbf{x})}{\partial\mathbf{q}} \tag{10} $$

It should be noted that the image Jacobian matrix is the matrix $\frac{1}{{}^{c}z}\mathbf{A}(\mathbf{q})$. Matrix **A(q)** differs from the image Jacobian matrix by the scale factor. Here we call **A(q)** *Depth-independent interaction matrix*. Note that in the matrix **A(q)** the coordinates vector **x** is a constant vector. The products of the components of the perspective project matrix **M** and the components of the vector **x** are in the linear form in the Depth-independent interaction matrix.

Proposition 1: Assume that the Jacobian matrix **J(q**(*t*)**)** of the manipulator is not singular. For any vector ${}^{b}\mathbf{x}$, the matrix $\frac{\partial(\mathbf{T}_{\mathbf{e}}^{-1}(t)\mathbf{x})}{\partial\mathbf{q}}$ has a rank of 3.

Proof: Substituting (10) into the matrix (9), we obtain

$$ \begin{aligned} \frac{\partial(\mathbf{T}_{\mathbf{e}}^{-1}(t)\mathbf{x})}{\partial\mathbf{q}} &= \frac{\partial\left(\mathbf{R}(t)^{b}\mathbf{x} + \xi(t)\right)}{\partial\mathbf{q}} \\ &= \left(sk\{\mathbf{R}(t)^{b}\mathbf{x} + \xi(t)\} \quad \mathbf{I}_{3\times3}\right)\begin{pmatrix} \mathbf{R}(t) & 0 \\ 0 & \mathbf{R}(t) \end{pmatrix}\mathbf{J}(\mathbf{q}(t)) \end{aligned} \tag{11} $$

where *sk* is a matrix operator and $sk(\mathbf{x})$ with vector $\mathbf{x} = \begin{bmatrix} x_1 & x_2 & x_3 \end{bmatrix}^T$ can be written as a matrix form

$$ sk(\mathbf{x}) = \begin{pmatrix} 0 & -x_3 & x_2 \\ x_3 & 0 & -x_1 \\ -x_2 & x_1 & 0 \end{pmatrix} \tag{12} $$

■

Obviously, the matrix in (11) has a rank of 3.

Proposition 2: *The Dept- independent interaction matrix* $\mathbf{A(q)}$ *has a rank of 2 if the matrix* $\mathbf{M}$ *is a perspective projection matrix.*

Proof: This proposition can be proved if we can show that the matrix $\mathbf{D}$ has a rank of 2. Assume that the rank of the matrix $\mathbf{D}$ is smaller than 2. Then, there exist nonzero scalars λ_1 and λ_2 such that

$$\lambda_1(\mathbf{m_1} - u\mathbf{m_3}) + \lambda_2(\mathbf{m_2} - v\mathbf{m_3}) = 0 \tag{13}$$

This equation can be written as

$$\lambda_1\mathbf{m_1} + \lambda_2\mathbf{m_2} - (\lambda_1 u + \lambda_2 v)\mathbf{m_3} = 0 \tag{14}$$

If $(\lambda_1 u + \lambda_2 v)$ is not zero, eq. (14) means that the row vectors of $\mathbf{M}$ are linearly dependent. If the coefficient is zero, the first two row vectors are linearly dependent. However, the row vectors must be linearly independent because the rank of $\mathbf{M}$ is 3. Therefore, the rank of the matrix $\mathbf{D}$ is 2. ■

Property 2: *For any vector* $\boldsymbol{\rho}$ *, the product* $\mathbf{A(q)\rho}$ *can be written as a linear form of the unknown parameters ,i.e.*

$$\mathbf{A(q)\rho = Q(\rho, q, y)\theta} \tag{15}$$

where $\mathbf{Q(\rho, q, y)}$ *does not depend on the parameters representing the products of the camera parameters and the world coordinates of the target point.*

2.3 Robot Dynamics

The dynamic equation of a robot manipulator has the form:

$$\mathbf{H(q)\ddot{q}} + (\frac{1}{2}\mathbf{\dot{H}(q)} + \mathbf{C(q, \dot{q})})\mathbf{\dot{q}} + \mathbf{G(q)} = \boldsymbol{\tau} \tag{16}$$

where $\mathbf{H(q)}$ is the positive-definite and symmetric inertia matrix. $\mathbf{C(q, \dot{q})}$ is a skew-symmetric matrix. The term $\mathbf{G(q)}$ represents the gravitational force, and $\boldsymbol{\tau}$ is the joint input of the robot manipulator. The first term on the left side of (16) is the inertial force, and the second term represents the Colioris and centrifugal forces.

3. Adaptive Image-based Visual Servoing with Unknown Target Positions

Our objective is to develop a controller that is able to estimate the unknown parameters on-line while controlling motion of the manipulator. This problem differs from traditional adaptive control utilizing state feedback errors. The feedback signals here are the image errors, which are outputs of the system. Fortunately, the state information of the manipulator can be also obtained by the internal sensors, so the problem is slightly different from output adaptive control problems in nonlinear control theory. We propose to employ a hybrid feedback scheme that feeds back both the position and velocity (state) of the manipulator and the image errors (output).

In this section, we assume that the world coordinates of the target point are unknown. Therefore the unknown parameters $\boldsymbol{\theta}$ here is only the three coordinate components of the target position $\mathbf{x}$.

3.1 Controller Design

Denote the desired position of the target point on the image plane by $\mathbf{y_d}$. The image error is given by:

$$\mathbf{\Delta y = y - y_d} \tag{17}$$

Denote an estimation of the unknown parameters $\boldsymbol{\theta}$ by $\hat{\boldsymbol{\theta}}$. Using the estimation, we propose the following controller:

$$\boldsymbol{\tau} = \mathbf{G(q) - K_1\dot{q} - (\hat{A}^T(q) + \frac{1}{2}\hat{n}(q)\Delta y^T)B\Delta y} \tag{18}$$

The first term is to cancel the gravitational force. The second term is a velocity feedback. The last term represents the visual feedback. $\mathbf{\hat{A}(q)}$ is the estimated Depth-independent interaction matrix calculated by the estimated parameters. $\mathbf{\hat{n}(q)}$ is an estimation of vector $\mathbf{n(q)}$, $\mathbf{K_1}$ and $\mathbf{B}$ are positive definite gain matrices. It is important to note that $\frac{1}{c_z}$ does not appear in the controller. The quadratic form of $\Delta\mathbf{y}$ is to compensate for the effect of the scale factor. Using the Depth-independent interaction matrix and including the quadratic term differentiates our controller from other existing ones. By substituting (18) into (16), we obtain:

$$\begin{aligned}\mathbf{H(q)\ddot{q} + (\frac{1}{2}\dot{H}(q) + C(q,\dot{q}))\dot{q} = -K_1\dot{q}} \\ \mathbf{-(A^T(q) + \frac{1}{2}n(q)\Delta y^T)B\Delta y - [(\hat{A}^T(q) - A^T(q)) + \frac{1}{2}(\hat{n}(q) - n)\Delta y^T]B\Delta y}\end{aligned} \tag{19}$$

From the Property 2, the last term can be represented as a linear form of the estimation errors of the parameters as follows:

$$\mathbf{-[(\hat{A}^T(q) - A^T(q)) + \frac{1}{2}(\hat{n}(q) - n)\Delta y^T]B\Delta y = Y(q,y)\Delta\theta} \tag{20}$$

where $\mathbf{\Delta\theta = \hat{\theta} - \theta}$ is the estimation error and the regressor $\mathbf{Y(q,y)}$ does not depend on the unknown parameters.

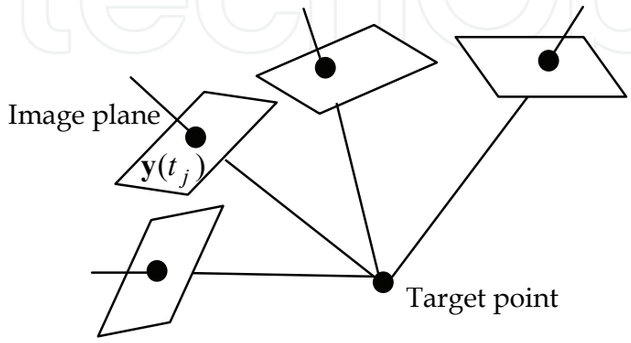

Figure 9. Projections of the target point on image planes

3.2 Estimation of the Parameters

With the motion of the robot manipulator, the camera moves and captures the images of the target point from different view points (Fig. 9). What we need to estimate is the 3-D coordinates of the target point. The problem is similar to the projective structure from motion problem in computer vision. However, it should be pointed out that there are two differences here: 1) only the initial parameters need to be estimated and the remaining can be obtained from motion of the manipulator and 2) the estimation must be conducted on-line. In the projective structure from motion, the basic idea is to find a solution of matrix **M** and **x** that minimizes the Frobenius norm given by

$$\mathbf{E} = \sum_{j=1}^{l} \left\| {}^{c}z\mathbf{y}(t_j) - \mathbf{M}\mathbf{T}_{\mathbf{e}}^{-1}(\mathbf{q}(t_j))\mathbf{x} \right\|^2 \tag{21}$$

where l denotes the number of images captured by the cameras at difference configurations of the manipulator. Here t_j represents the time instant when the j-th image was captured. $\mathbf{y}(t_j) = (u(t_j), v(t_j), 1)^T$ is image coordinates of the target point on the j-th image and $\mathbf{q}(t_j)$ represents the corresponding joint angles. Note that the l images can be selected from the trajectory of camera. By substituting the estimated parameters in the Frobenius norm, we note that

$$\begin{aligned} & {}^{c}\hat{z}(t_j)\mathbf{y}(t_j) - \mathbf{M}\mathbf{T}_{\mathbf{e}}^{-1}\hat{\mathbf{x}} \\ &= \mathbf{y}(t_j)({}^{c}\hat{z}(t_j) - {}^{c}z(t_j)) - (\mathbf{M}\mathbf{T}_{\mathbf{e}}^{-1}\hat{\mathbf{x}} - \mathbf{M}\mathbf{T}_{\mathbf{e}}^{-1}\mathbf{x}) \\ &= \mathbf{W}(\mathbf{x}(t_j), \mathbf{y}(t_j))\Delta\boldsymbol{\theta} \end{aligned} \tag{22}$$

From the result in computer vision, we have

Proposition 3*: If 2 images are selected from the trajectory of the camera, the equation*

$$\mathbf{W}(\mathbf{x}(t_j), \mathbf{y}(t_j))\Delta\boldsymbol{\theta} = 0, \quad \forall j = 1,2 \tag{23}$$

implies the estimated parameters can be estimated to the real values up to a scale..

Based on the discussion above, we propose the following adaptive rule:

$$\frac{d}{dt}\hat{\boldsymbol{\theta}} = -\boldsymbol{\Gamma}^{-1}\{\mathbf{Y}^{\mathbf{T}}(\mathbf{q},\mathbf{y})\dot{\mathbf{q}} + \sum_{j=1}^{l}\mathbf{W}^{\mathbf{T}}(\mathbf{x}(t_j), \mathbf{y}(t_j))\mathbf{K}_{\mathbf{3}}\mathbf{W}(\mathbf{x}(t_j), \mathbf{y}(t_j))\Delta\boldsymbol{\theta}\} \tag{24}$$

where $\boldsymbol{\Gamma}$ and $\mathbf{K}_{\mathbf{3}}$ are positive-definite and diagonal gain matrices. To simplify the notation, let

$$\mathbf{W}_{\mathbf{j}} = \mathbf{W}(\mathbf{x}(t_j), \mathbf{y}(t_j)) \tag{25}$$

Remark 1: *The adaptive algorithm (24) differs from Slotine and Li's algorithm (Slotine &Li, 1987) due to the existence of the last term and the potential force, which ensures the convergence of the estimated parameters to real values.*

3.3 Stability Analysis

This section analyses the stability of the proposed controller.

Theorem 1*: Under the control of the controller (18) and the adaptive algorithm (24) for parameters estimation, the image error of the target point is convergent to zero, i.e.*

$$\lim_{t\to\infty} \Delta\mathbf{y} = 0 \tag{26}$$

Furthermore, if a sufficient number of images are used in the adaptive algorithm, the estimated parameters are convergent to the real ones up to a scale.

Proof: Introduce the following positive function:

$$V(t) = \frac{1}{2}\{\dot{\mathbf{q}}^{\mathbf{T}}\mathbf{H}(\mathbf{q})\dot{\mathbf{q}} + {}^{c}z\Delta\mathbf{y}^{\mathbf{T}}\mathbf{B}\Delta\mathbf{y} + \Delta\boldsymbol{\theta}^{\mathbf{T}}\boldsymbol{\Gamma}\Delta\boldsymbol{\theta}\} \tag{27}$$

Notice that ${}^{c}z > 0$. Multiplying the $\dot{\mathbf{q}}^{\mathbf{T}}$ from the left to (19) results in

$$\dot{\mathbf{q}}^{\mathbf{T}}\mathbf{H}(\mathbf{q})\ddot{\mathbf{q}} + \frac{1}{2}\dot{\mathbf{q}}^{\mathbf{T}}\dot{\mathbf{H}}(\mathbf{q})\dot{\mathbf{q}} = -\dot{\mathbf{q}}^{\mathbf{T}}\mathbf{K}_{\mathbf{1}}\dot{\mathbf{q}} - \dot{\mathbf{q}}^{\mathbf{T}}\mathbf{A}^{\mathbf{T}}(\mathbf{q})\mathbf{B}\Delta\mathbf{y} - \frac{1}{2}\dot{\mathbf{q}}^{\mathbf{T}}\mathbf{n}(\mathbf{q})(\Delta\mathbf{y}^{\mathbf{T}}\mathbf{B}\Delta\mathbf{y}) + \dot{\mathbf{q}}^{\mathbf{T}}\mathbf{Y}(\mathbf{q},\mathbf{y})\Delta\boldsymbol{\theta} \tag{28}$$

From equation (9), we have

$$\dot{\mathbf{q}}^{\mathbf{T}}\mathbf{A}^{\mathbf{T}}(\mathbf{q}) = {}^{c}z\dot{\mathbf{y}}^{\mathbf{T}} = {}^{c}z\Delta\dot{\mathbf{y}}^{\mathbf{T}} \tag{29}$$

Multiplying the $\Delta\boldsymbol{\theta}^{\mathbf{T}}$ from the left to (24), we obtain

$$\Delta\boldsymbol{\theta}^{\mathbf{T}}\boldsymbol{\Gamma}\Delta\dot{\boldsymbol{\theta}} = -\Delta\boldsymbol{\theta}^{\mathbf{T}}\mathbf{Y}^{\mathbf{T}}(\mathbf{q},\mathbf{y})\dot{\mathbf{q}} - \sum_{j=1}^{l}\Delta\boldsymbol{\theta}^{\mathbf{T}}\mathbf{W}_{\mathbf{j}}^{\mathbf{T}}\mathbf{K}_{\mathbf{3}}\mathbf{W}_{\mathbf{j}}\Delta\boldsymbol{\theta} \tag{30}$$

Differentiating the function *V(t)* results in

$$\dot{V}(t) = \dot{\mathbf{q}}^{\mathbf{T}}(\mathbf{H}(\mathbf{q})\ddot{\mathbf{q}} + \frac{1}{2}\dot{\mathbf{H}}(\mathbf{q}))\dot{\mathbf{q}} + \Delta\dot{\boldsymbol{\theta}}^{\mathbf{T}}\boldsymbol{\Gamma}\Delta\boldsymbol{\theta} + {}^{c}z\Delta\dot{\mathbf{y}}^{\mathbf{T}}\mathbf{B}\Delta\mathbf{y} + \frac{1}{2}{}^{c}\dot{z}\Delta\mathbf{y}^{\mathbf{T}}\mathbf{B}\Delta\mathbf{y} \tag{31}$$

Note that

$${}^{c}\dot{z} = \mathbf{n}^{\mathbf{T}}\dot{\mathbf{q}} \tag{32}$$

By combining the equations (28)-(32), we have

$$\dot{V}(t) = -\dot{\mathbf{q}}^{\mathbf{T}}\mathbf{K}_{\mathbf{1}}\dot{\mathbf{q}} - \sum_{j=1}^{l}\Delta\boldsymbol{\theta}^{\mathbf{T}}\mathbf{W}_{\mathbf{j}}^{\mathbf{T}}\mathbf{K}_{\mathbf{3}}\mathbf{W}_{\mathbf{j}}\Delta\boldsymbol{\theta} \tag{33}$$

obviously we have $\dot{V}(t) \le 0$, and hence $\dot{\mathbf{q}}$, $\Delta\mathbf{y}$ and $\Delta\boldsymbol{\theta}$ are all bounded. From (19) and (24), we know $\ddot{\mathbf{q}}$ and $\dot{\hat{\boldsymbol{\theta}}}$ are bounded respectively. Differentiating the function $\dot{V}(t)$ resulting in

$$\ddot{V}(t) = -\ddot{\mathbf{q}}^{\mathbf{T}}\mathbf{K}_{\mathbf{1}}\dot{\mathbf{q}} - \sum_{j=1}^{l}(\Delta\dot{\boldsymbol{\theta}}^{\mathbf{T}}\mathbf{W}_{\mathbf{j}}^{\mathbf{T}} + \Delta\boldsymbol{\theta}^{\mathbf{T}}\dot{\mathbf{W}}_{\mathbf{j}}^{\mathbf{T}})\mathbf{K}_{\mathbf{3}}\mathbf{W}_{\mathbf{j}}\Delta\boldsymbol{\theta} \tag{34}$$

Then, we can conclude that $\ddot{V}(t)$ is bounded. Consequently, from barbalat's lemma, we have

$$\begin{aligned} &\lim_{t\to\infty}\dot{\mathbf{q}} = 0 \\ &\lim_{t\to\infty}\dot{\hat{\boldsymbol{\theta}}} = 0 \\ &\lim_{t\to\infty}\mathbf{W}(x(t_j), y(t_j))\Delta\boldsymbol{\theta} = 0 \end{aligned} \tag{35}$$

The convergence of $\mathbf{W_j}\Delta\boldsymbol{\theta}$ implies that the estimated matrix $\hat{\boldsymbol{\theta}}$ is convergent to the real values up to a scale. In order to prove the convergence of the image error, consider the invariant set of the system when $\dot{V}(t)=0$. From the close loop dynamics (19), at the invariant set,

$$(\hat{\mathbf{A}}^{\mathbf{T}}+\frac{1}{2}\hat{\mathbf{n}}\Delta\mathbf{y}^{\mathbf{T}})\mathbf{B}\Delta\mathbf{y}=0 \tag{36}$$

It is reasonable to assume that the manipulator is not at the singular configurations so that $\mathbf{J(q)}$ is of full rank. Note that

$$\hat{\mathbf{A}}^{\mathbf{T}}+\frac{1}{2}\hat{\mathbf{n}}\Delta\mathbf{y}^{\mathbf{T}}=\left[\frac{\partial(\mathbf{T_e^{-1}(q)}\hat{\mathbf{x}})}{\partial\mathbf{q}}\right]^{T}\underbrace{\begin{pmatrix}\mathbf{m_1^T}+(0.5\Delta u-u)\mathbf{m_3^T}\\ \mathbf{m_2^T}+(0.5\Delta v-v)\mathbf{m_3^T}\\ 0\end{pmatrix}^{T}}_{\mathbf{E}} \tag{37}$$

Since it is guaranteed that $\hat{\mathbf{x}}\neq 0$ at the invariant set, the matrix $\frac{\partial(\mathbf{T_e^{-1}(q)}\hat{\mathbf{x}})}{\partial\mathbf{q}}$ is not singular from Proposition 1. Then we proposed

Proposition 4: *The matrix* $\hat{\mathbf{A}}^{\mathbf{T}}+\frac{1}{2}\hat{\mathbf{n}}\Delta\mathbf{y}^{\mathbf{T}}$ *has a rank of 2 if the matrix* $\hat{\mathbf{M}}$ has a rank of 3.

This proposition can be proved if we can show that the matrix **E** has a rank of 2. the proof is similar to Proposition 2.

Therefore, from (36), it is obvious that at the invariant set the position error on the image plane must be zero, e.g.

$$\Delta\mathbf{y}=0 \tag{38}$$

From the Barbalat's lemma, we can conclude the convergence of the position error of the target point projections on the image plane to zero and convergence of the estimated parameters to the real values

4. Adaptive Image-based Visual Servoing with Unknown Camera Parameters and Target Positions

In this section, we assume that in addition to the 3-D coordinates of the target points, the intrinsic and extrinsic parameters of the camera are also unknown. Denote all the possible products of the components of matrix **M** and vector **x** by a vector $\boldsymbol{\theta}_l$, which represents all the unknown parameters including the camera intrinsic and extrinsic parameters and the unknown world coordinates of the target point. It should be pointed out that there are 39 unknown parameters in total. Here we fixed one parameters $\hat{p}_z=1$ and define the left 38 parameters as uniform parameters. Here we define $\hat{\boldsymbol{\theta}}_l=\frac{\hat{m}_{ij}\hat{x}_k}{\hat{p}_z}$ and $\boldsymbol{\theta}_l=\frac{m_{ij}x_k}{p_z}$, where

$$\forall\, l=1,...,38;\ i,j=1,2,3,\ k=1,2,3,4 \text{ or } i=1,2,\ j,k=4\,.$$

4.1 Controller Design

Using the estimation, we propose the following controller similar to the previous section:

$$\boldsymbol{\tau} = \mathbf{G}(\mathbf{q}) - \mathbf{K}_1\dot{\mathbf{q}} - (\hat{\mathbf{A}}^{\mathbf{T}}(\mathbf{q}) + \frac{1}{2}\hat{\mathbf{n}}(\mathbf{q})\Delta\mathbf{y}^{\mathbf{T}})\mathbf{B}\Delta\mathbf{y} \tag{39}$$

By substituting (39) into (16), we obtain:

$$\begin{aligned}\mathbf{H}(\mathbf{q})\ddot{\mathbf{q}} + (\frac{1}{2}\dot{\mathbf{H}}(\mathbf{q}) + \mathbf{C}(\mathbf{q},\dot{\mathbf{q}}))\dot{\mathbf{q}} &= -\mathbf{K}_1\dot{\mathbf{q}} \\ -(\frac{\mathbf{A}^{\mathbf{T}}(\mathbf{q})}{p_z} + \frac{1}{2}\frac{\mathbf{n}(\mathbf{q})\Delta\mathbf{y}^{\mathbf{T}}}{p_z})\mathbf{B}\Delta\mathbf{y} &- [(\hat{\mathbf{A}}(\mathbf{q}) - \frac{\mathbf{A}^{\mathbf{T}}(\mathbf{q})}{p_z}) + \frac{1}{2}(\hat{\mathbf{n}}(\mathbf{q}) - \frac{\mathbf{n}}{p_z})\Delta\mathbf{y}^{\mathbf{T}}]\mathbf{B}\Delta\mathbf{y}\end{aligned} \tag{40}$$

From the Property 2, the last term can be represented as a linear form of the estimation errors of the parameters as follows:

$$-[(\hat{\mathbf{A}}(\mathbf{q}) - \frac{\mathbf{A}^{\mathbf{T}}(\mathbf{q})}{p_z}) + \frac{1}{2}(\hat{\mathbf{n}}(\mathbf{q}) - \frac{\mathbf{n}}{p_z})\Delta\mathbf{y}^{\mathbf{T}}]\mathbf{B}\Delta\mathbf{y} = \mathbf{Y}(\mathbf{q},\mathbf{y})\Delta\boldsymbol{\theta}_l \tag{41}$$

where $\Delta\boldsymbol{\theta}_l = \hat{\boldsymbol{\theta}}_l - \boldsymbol{\theta}_l$ is the estimation error and the regressor $\mathbf{Y}(\mathbf{q},\mathbf{y})$ does not depend on the unknown parameters.

4.2 Estimation of the Parameters

The idea is same as previous section, we minimizes the Frobenius norm, Since there are 38 unknowns in $\boldsymbol{\theta}_l$, 19 images are necessary for estimating the parameters. By substituting the estimated parameters in the Frobenius norm, we note that

$$\begin{aligned}&{}^c\hat{z}(t_j)\mathbf{y}(t_j) - \hat{\mathbf{M}}\mathbf{T}_\mathbf{e}^{-1}\hat{\mathbf{x}} \\ &= \mathbf{y}(t_j)({}^c\hat{z}(t_j) - \frac{{}^c z(t_j)}{p_z}) - (\hat{\mathbf{M}}\mathbf{T}_\mathbf{e}^{-1}\hat{\mathbf{x}} - \frac{\mathbf{M}\mathbf{T}_\mathbf{e}^{-1}\mathbf{x}}{p_z}) \\ &= \mathbf{W}(\mathbf{x}(t_j),\mathbf{y}(t_j))\Delta\boldsymbol{\theta}_l\end{aligned} \tag{42}$$

From the result in computer vision, we have

Proposition 5: *If a sufficient number of images are selected from the trajectory of the camera, then*

$$\mathbf{W}(\mathbf{x}(t_j),\mathbf{y}(t_j))\Delta\boldsymbol{\theta} = 0, \quad \forall j = 1,2,...,l \tag{43}$$

implies one of the following two cases:

(1) the estimated parameters can be estimated to the real values up to a scale, i.e.

$$\hat{\boldsymbol{\theta}} = \lambda\boldsymbol{\theta} \tag{44}$$

By the definition of $\boldsymbol{\theta}_l$, *we can estimate the perspective projection matrix to the real one up to a scale.*

$$\hat{\mathbf{M}} = \lambda\mathbf{M} \tag{45}$$

then matrix $\hat{\mathbf{M}}$ *a rank of 3 from Property 1.*

(2) The estimated parameters are zero.

Proposition 6*: If* $\mathbf{W}(\mathbf{x}(t_j),\mathbf{y}(t_j))\Delta\boldsymbol{\theta}_l = 0$, *we can avoid the trivial solution of* $\hat{\boldsymbol{\theta}}_l = 0$.

Proof: By fixing the parameter $\hat{p}_z = 1$, if $\hat{\boldsymbol{\theta}}_l = 0$, we can obtain ${}^c\hat{z} = \hat{\mathbf{m}}_3^{\mathbf{T}}\mathbf{T_e^{-1}(q)}\hat{\mathbf{x}} = 1$, which implies that $\mathbf{W}(\mathbf{x}(t_j),\mathbf{y}(t_j))\Delta\boldsymbol{\theta}_l = \mathbf{y}(t_j)$. It is obviously wrong since we know that $\mathbf{W}(\mathbf{x}(t_j),\mathbf{y}(t_j))\Delta\boldsymbol{\theta}_l = 0$. So we can avoid the trivial solution.

Remark 2: By Proposition 6 and (44), it is easy to guaranteed that $\hat{\mathbf{x}} \neq 0$.
The adaptive rule is simlar as (24)

$$\frac{d}{dt}\hat{\boldsymbol{\theta}}_l = -\boldsymbol{\Gamma}^{-1}\{\mathbf{Y^T(q,y)}\dot{\mathbf{q}} + \sum_{j=1}^{l}\mathbf{W^T}(\mathbf{x}(t_j),\mathbf{y}(t_j))\mathbf{K_3}\mathbf{W}(\mathbf{x}(t_j),\mathbf{y}(t_j))\Delta\boldsymbol{\theta}_l\} \tag{46}$$

4.3 Stability Analysis

This section analyses the stability of the proposed controller.

Theorem 2*: Under the control of the controller (39) and the adaptive algorithm (46) for parameters estimation, the image error of the target point is convergent to zero, i.e.*

$$\lim_{t\to\infty}\Delta\mathbf{y} = 0 \tag{47}$$

Furthermore, the estimated parameters are convergent to the real values up to a scale:

Proof: Introduce the following positive function:

$$V(t) = \frac{1}{2}\{\dot{\mathbf{q}}^{\mathbf{T}}\mathbf{H(q)}\dot{\mathbf{q}} + \frac{{}^c z}{p_z}\Delta\mathbf{y}^{\mathbf{T}}\mathbf{B}\Delta\mathbf{y} + \Delta\boldsymbol{\theta}^{\mathbf{T}}\boldsymbol{\Gamma}\Delta\boldsymbol{\theta}\} \tag{48}$$

Notice that $p_z > 0$ and ${}^c z > 0$. Multiplying the $\dot{\mathbf{q}}^{\mathbf{T}}$ from the left to (19) results in

$$\begin{aligned}\dot{\mathbf{q}}^{\mathbf{T}}\mathbf{H(q)}\ddot{\mathbf{q}} + \frac{1}{2}\dot{\mathbf{q}}^{\mathbf{T}}\dot{\mathbf{H}}\mathbf{(q)}\dot{\mathbf{q}} &= -\dot{\mathbf{q}}^{\mathbf{T}}\mathbf{K_1}\dot{\mathbf{q}} - \frac{1}{p_z}\dot{\mathbf{q}}^{\mathbf{T}}\mathbf{A^T(q)B}\Delta\mathbf{y} \\ &- \frac{1}{2p_z}\dot{\mathbf{q}}^{\mathbf{T}}\mathbf{n(q)}(\Delta\mathbf{y}^{\mathbf{T}}\mathbf{B}\Delta\mathbf{y}) + \dot{\mathbf{q}}^{\mathbf{T}}\mathbf{Y(q,y)}\Delta\boldsymbol{\theta}_l\end{aligned} \tag{49}$$

Differentiating the function *V(t)* results in

$$\dot{V}(t) = \dot{\mathbf{q}}^{\mathbf{T}}(\mathbf{H(q)}\ddot{\mathbf{q}} + \frac{1}{2}\dot{\mathbf{H}}\mathbf{(q)})\dot{\mathbf{q}} + \Delta\dot{\boldsymbol{\theta}}^{\mathbf{T}}\boldsymbol{\Gamma}\Delta\boldsymbol{\theta} + \frac{{}^c z}{p_z}\Delta\dot{\mathbf{y}}^{\mathbf{T}}\mathbf{B}\Delta\mathbf{y} + \frac{1}{2p_z}{}^c\dot{z}\Delta\mathbf{y}^{\mathbf{T}}\mathbf{B}\Delta\mathbf{y} \tag{50}$$

By proper simplification, we have

$$\dot{V}(t) = -\dot{\mathbf{q}}^{\mathbf{T}}\mathbf{K_1}\dot{\mathbf{q}} - \sum_{j=1}^{l}\Delta\boldsymbol{\theta}^{\mathbf{T}}\mathbf{W_j^T}\mathbf{K_3}\mathbf{W_j}\Delta\boldsymbol{\theta}_l \tag{51}$$

obviously we have $\dot{V}(t) \le 0$, and hence $\dot{\mathbf{q}}$, $\Delta\mathbf{y}$ and $\Delta\boldsymbol{\theta}_l$ are all bounded. From (19) and (46), we know $\ddot{\mathbf{q}}$ and $\dot{\hat{\boldsymbol{\theta}}}_l$ are bounded respectively. Differentiating the function $\dot{V}(t)$ resulting in

$$\ddot{V}(t) = -\ddot{\mathbf{q}}^{\mathbf{T}}\mathbf{K_1}\dot{\mathbf{q}} - \sum_{j=1}^{l}(\Delta\dot{\boldsymbol{\theta}}^{\mathbf{T}}\mathbf{W_j^T} + \Delta\boldsymbol{\theta}^{\mathbf{T}}\dot{\mathbf{W}}_{\mathbf{j}}^{\mathbf{T}})\mathbf{K_3}\mathbf{W_j}\Delta\boldsymbol{\theta}_l \tag{52}$$

Similar as Theorem 1, From the Barbalat's lemma, we can conclude the convergence of the position error of the target point projections on the image plane to zero and convergence of the estimated parameters to the real values.

4.4 Extension to Multiple Feature Points

This controller can be directly extended to visual seroving using a number S of feature points. In control of multiple feature points, the dimension of the depth independent interaction matrix will increase, and hence the major difference will be the difference in computation time. A controller similar to that in (39) can be designed by

$$\boldsymbol{\tau} = \mathbf{G}(\mathbf{q}(t)) - \mathbf{K}_1\dot{\mathbf{q}}(t) - \sum_{i=1}^{S}(\hat{\mathbf{A}}_i^T(t) + \frac{1}{2}\hat{\mathbf{n}}_i(t)\Delta\mathbf{y}_i^T(t))\mathbf{B}\Delta\mathbf{y}_i(t) \tag{53}$$

where $\hat{\mathbf{A}}_i(t)$ and $\hat{\mathbf{n}}_i(t)$ have a similar form to Eq. (10) and Eq. (7) for point i, respectively. $\Delta\mathbf{y}_i(t)$ is the image position error for i-th feature point. The image errors are convergent to zero when the number n of degrees of freedom of the manipulator is larger than or equal to $2S$.

When n=6 and $S \geq 3$, the convergence of image errors can also be guaranteed. It is well known that three non-collinear projections of fixed feature points on the image plane can uniquely define the 3-D position of the camera, and hence the projections of all other fixed feature points are uniquely determined. Therefore, if the projections of three feature points whose projections are convergent to their desired positions on the image plane, so are the projection of all other feature points. We can conclude the convergence of the image errors when the manipulator has equal or more degrees of freedom than $2S$, or when the manipulator has 6 degrees of freedom.

5. Experiments

We have implemented the controller in a 3 DOF robot manipulator in the Chinese University of Hong Kong. Fig. 10 shows the experiment setup system. The moment inertia about its vertical axis of the first link of the manipulator is 0.005kgm^2, the masses of the second and third links are 0.167 kg, and 0.1 kg, respectively. The lengths of the second and third links are, 0.145m and 0.1285m, respectively. The joints of the manipulator are driven by Maxon brushed DC motors. The powers of the motors are 20 watt, 10 watt, and 10watt, respectively. The gear ratios at the three joints are 480:49, 12:1, and 384:49, respectively. High-precision Encoders are used to measure the joint angles. The joint velocities are obtained by differentiating the joint angles. A frame processor MATROX PULSAR installed in a PC with Intel Pentium II CPU acquires the video signal. This PC processes the image and extracts the image features.

5.1 Control of One Feature Point with Unknown Target Positions

We first set initial positions and record the image position of the point and then move the end-effector to another position and record that image position as the desired ones (Fig. 11). The control gains are $\mathbf{K}_1 = 30$, $\mathbf{B} = 0.00006$, $\mathbf{K}_3 = 0.001$, $\boldsymbol{\Gamma} = 5000$. The transformation

matrix of the base frame respect to the vision frame is $\mathbf{T} = \begin{bmatrix} 0 & 0 & 1 & 0 \\ 0 & -1 & 0 & 0 \\ 1 & 0 & 0 & 1 \\ 0 & 0 & 0 & 1 \end{bmatrix}$, the initial estimated target position is $\mathbf{x} = [0.85 \quad -0.15 \quad 0.05]^T$. The real camera intrinsic parameters are $a_u = 871$, $a_v = 882$, $u_0 = 381$, $v_0 = 278$.

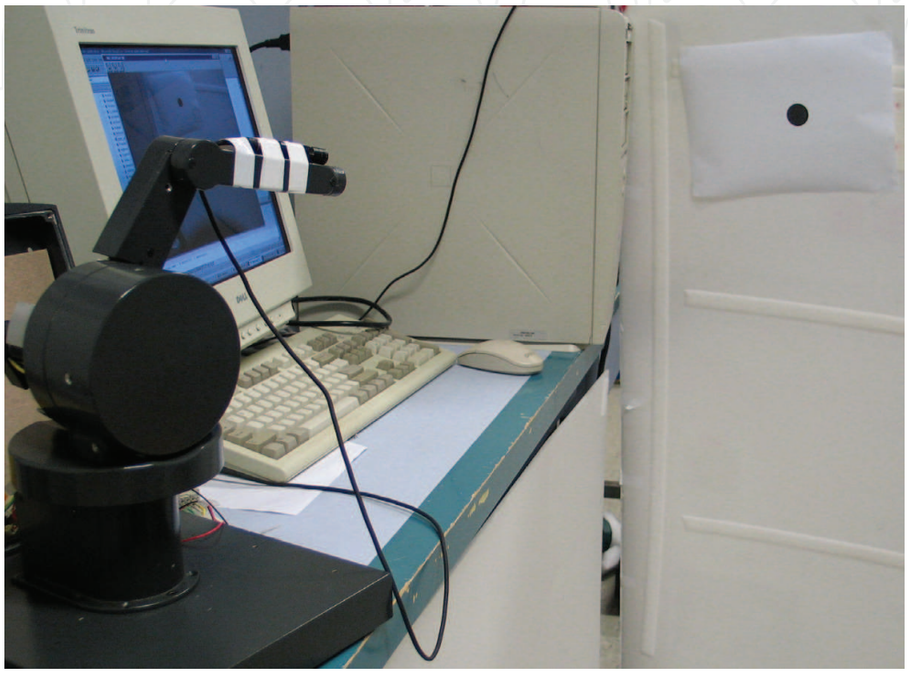

Figure 10. The experiment setup system

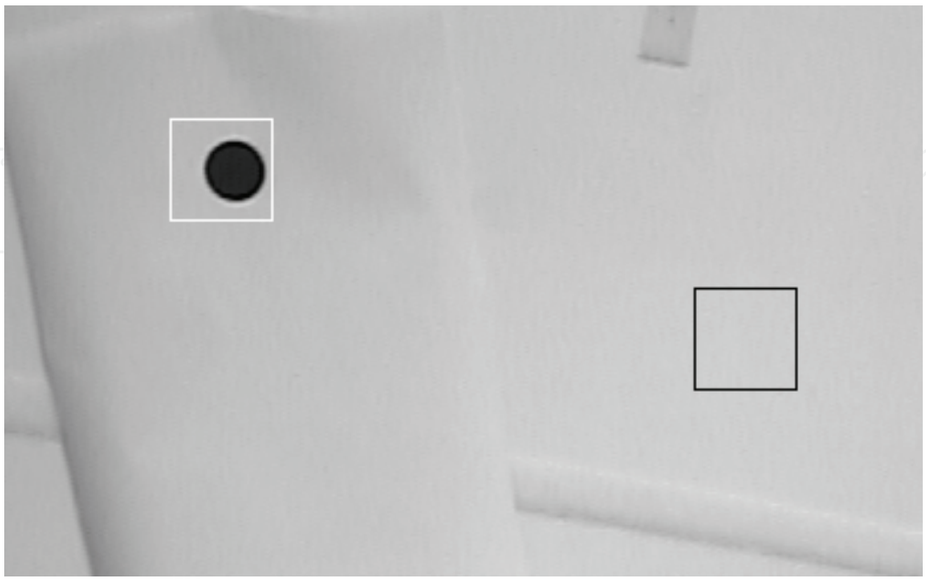

Figure 11. The initial and desired (black square) positions

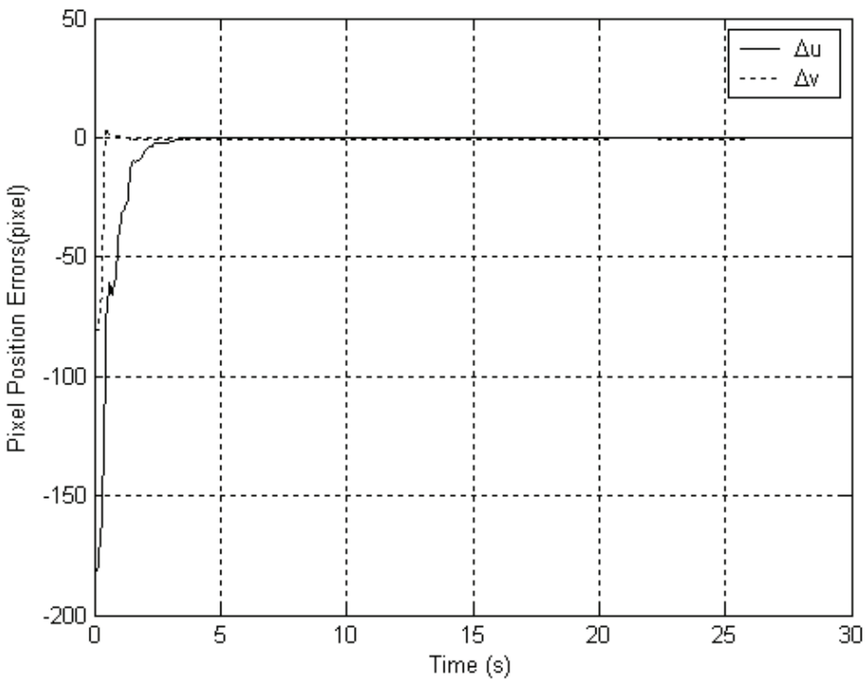

Figure 12. Position errors of the image feature

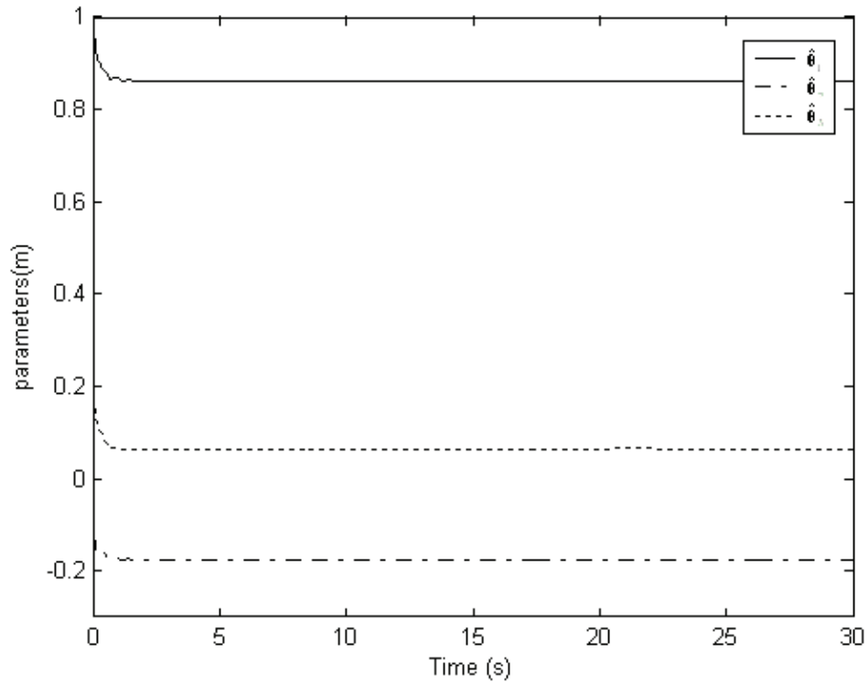

Figure 13. The profile of the estimated parameters

As shown in Fig. 12, the image feature points asymptotically converge to the desired ones. The results confirmed the convergence of the image error to zero under control of the proposed method. Fig. 13 plots the profiles of the estimated parameters, which are not convergent to the true values. The sampling time in the experiment is 40ms.

5.2 Control of One Feature Point with Unknown Camera Parameters and Target Positions

The initial and final positions are same as Fig. 10. The control gains are the same as previous experiments. The initial estimated transformation matrix of the base frame respect to the vision frame is $\hat{\mathbf{T}} = \begin{bmatrix} -0.3 & 0 & 0.95 & 0 \\ 0 & -1 & 0 & 0 \\ 0.95 & 0 & 0.3 & 1 \\ 0 & 0 & 0 & 1 \end{bmatrix}$, The initial estimated target position is $\hat{\mathbf{x}} = [1 \quad -0.1 \quad 0.2]^T$ m. The estimated intrinsic parameters are $\hat{a}_u = 1000$, $\hat{a}_v = 1000$, $\hat{u}_0 = 300$, $\hat{v}_0 = 300$. The image errors of the feature points on the image plane are demonstrated in Fig. 14. Fig. 15 plots the profiles of the estimated parameters.

This experiment showed that it is possible to achieve the convergence without camera parameters and target position information, by using the adaptive rule.

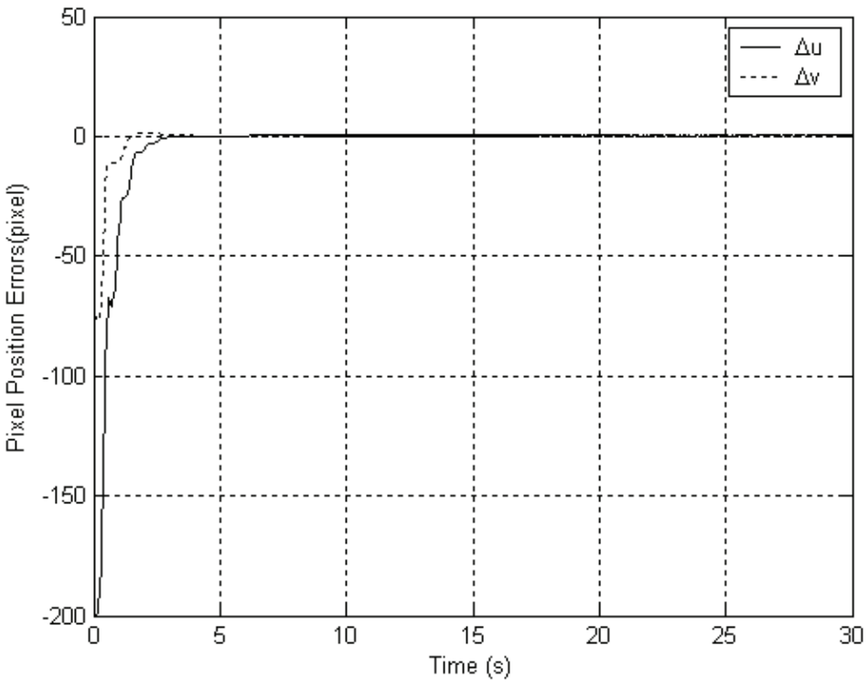

Figure 14. Position errors of the image feature

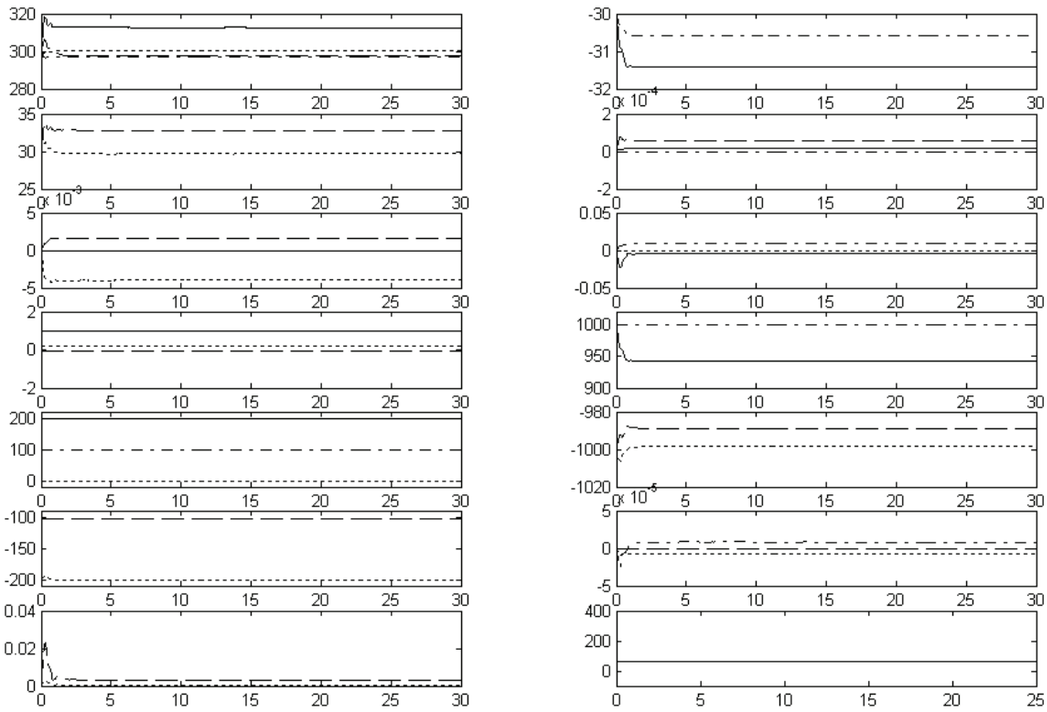

Figure 15. The profile of the estimated parameters

5.3 Control of Three Feature Points

In the third experiment, we control three feature points whose coordinates with respect to the end-effector frames are $\hat{\mathbf{x}}_1 = [1 \quad -0.1 \quad 0.2]^T$ m, $\hat{\mathbf{x}}_2 = [1 \quad -0.15 \quad 0.25]^T$ m, and $\hat{\mathbf{x}}_3 = [1 \quad -0.15 \quad 0.15]^T$ m, respectively.

The initial and desired positions of the feature points are shown in Fig. 16. The image errors of the feature points on the image plane are demonstrated in Fig. 17. The experimental results confirmed that the image errors of the feature points are convergent to zero. The residual image errors are within one pixel. In this experiment, we employed three current positions of the feature points in the adaptive rule. The control gains used the experiments are $\mathbf{K_1} = 18$, $\mathbf{B} = 0.000015$, $\mathbf{K_3} = 0.001$, $\mathbf{\Gamma} = 10000$. The true values and initial estimations of the camera intrinsic and extrinsic parameters are as the same as those in previous experiments.

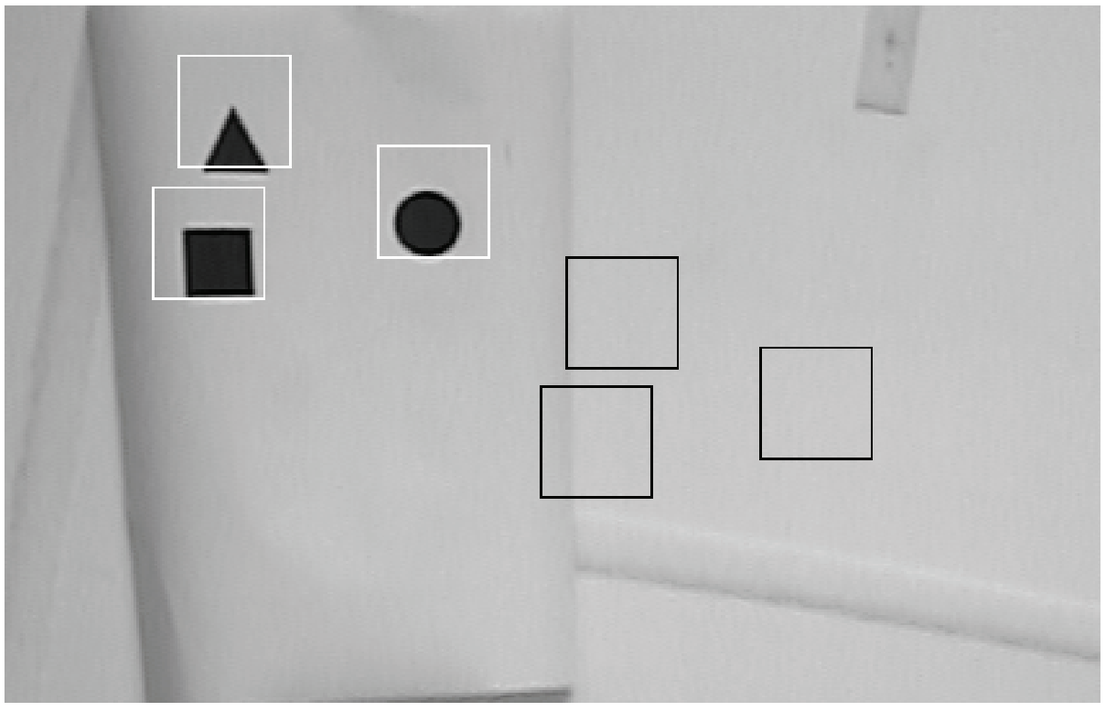

Figure 16. The initial and desired (black square) positions

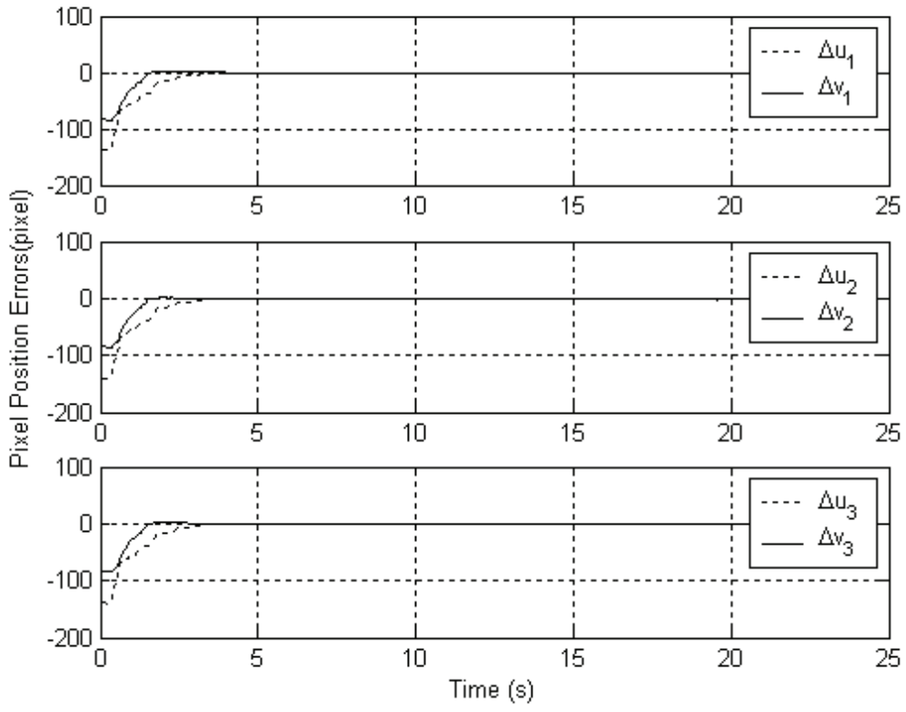

Figure 17. Position errors of the image features

6. Conclusion

This Chapter presents a new adaptive controller for dynamic image-based visual servoing of a robot manipulator uncalibrated eye-in-hand visual feedback. To cope with nonlinear dependence of the image Jacobian on the unknown parameters, this controller employs a matrix called depth-independent interaction matrix which does not depend on the scale factors determined by the depths of target points. A new adaptive algorithm has been developed to estimate the unknown intrinsic and extrinsic parameters and the unknown 3-D coordinates of the target points. With a full consideration of dynamic responses of the robot manipulator, we employed the Lyapunov method to prove the convergence of the postion errors to zero and the convergence of the estimated parameters to the real values. Experimental results illustrate the performance of the proposed methods.

7. References

Bishop. B. & Spong. M.W. (1997). Adaptive Calibration and Control of 2D Monocular Visual Servo System, *Proc. of IFAC Symp. Robot Control*, pp. 525-530.

Carelli. R.; Nasisi. O. & Kuchen. B. (1994). Adaptive robot control with visual feedback, *Proc. of the American Control Conf.*, pp. 1757-1760.

Cheah. C C.; Hirano. M.; Kawamura. S. & Arimoto. S. (2003). Approximate Jacobian control for robots with uncertain kinematics and dynamics, *IEEE Transactions on Robotics and Automation*, vol. 19, no. 4, pp. 692 – 702.

Deng. L.; Janabi-Sharifi. F. & Wilson. W. J. (2002). Stability and robustness of visual servoing methods, *Prof. of IEEE Int. Conf. on Robotics and Automation,* pp. 1604 – 1609.

Dixon. W. E. (2007). Adaptive regulation of amplitude limited robot manipulators with uncertain kinematics and dynamics," *IEEE Trans. on Automatic Control*, vol. 52, no. 3, pp. 488 --493.

Hashitmoto. K.; Nagahama. K. & Noritsugu. T. (2002). A mode switching estimator for visual seroving, *Proc. of IEEE Int. Conf. on Robotics and Automation,* pp. 1610- 1615.

Hemayed. E. E. (2003). A survey of camera self-calibration, *Proc. IEEE Conf. on Advanced Video and Signal Based Surveillance,* pp. 351-357.

Hosada. K. & Asada. M. (1994). Versatile Visual Servoing without knowledge of True Jacobain, *Proc. of IEEE/RSJ Int. Conf. on Intelligent Robots and Systems*, pp.186-191.

Hsu. L. & Aquino. P. L. S. (1999). Adaptive visual tracking with uncertain manipulator dynamics and uncalibrated camera, *Proc. of the 38th IEEE Int. Conf. on Decision and Control*, pp. 1248-1253.

Hutchinson. S.; Hager. G. D. & Corke. P. I. (1996). A tutorial on visual servo control, *IEEE Trans. on Robotics and Automation,* vol. 12, no. 5, pp. 651-670.

Kelly. R.; Reyes. F.; Moreno. J. & Hutchinson. S. (1999). A two-loops direct visual control of direct-drive planar robots with moving target, *Proc. of IEEE Int. Conf. on Robotics and Automation*, pp. 599-604.

Kelly. R.; Carelli. R.; Nasisi. O.; Kuchen. B. & Reyes. F. (2000). Stable Visual Servoing of Camera-in-Hand Robotic Systems, *IEEE/ASME Trans. on Mechatronics*, Vol. 5, No.1, pp.39-48.

Liu. Y. H.; Wang. H. & Lam. K. (2005). Dynamic visual servoing of robots in uncalibrated environments, *Proc. of IEEE Int. Conf. on Robotics and Automation*, pp. 3142-3147.

Liu. Y. H.; Wang. H.; Wang. C. & Lam. K. (2006). Uncalibrated Visual Servoing of Robots Using a Depth-Independent Image Jacobian Matrix, *IEEE Trans. on Robotics*, Vol. 22, No. 4.

Liu. Y. H.; Wang. H. & Zhou. D. (2006). Dynamic Tracking of Manipulators Using Visual Feedback from an Uncalibrated Fixed Camera, *Proc. of IEEE Int. Conf. on Robotics and Automation*, pp.4124-4129.

Malis. E.; Chaumette. F. & Boudet S. (1999). 2-1/2-D Visual Servoing, *IEEE Transaction on Robotics and Automation*, vol. 15, No. 2.

Malis E. (2004). Visual servoing invariant to changes in camera-intrisic parameters, *IEEE.Trans. on Robotics and Automation*, vol. 20, no.1, pp. 72-81.

Nagahama. K.; Hashimoto. K.; Norisugu. T. & Takaiawa. M. (2002). Visual servoing based on object motion estimation, *Proc. IEEE Int. Conf. on Robotics and Automation*, pp. 245-250.

Papanikolopoulos. N. P.; Nelson. B. J. & Khosla. P. K. (1995). Six degree-of-freedom hand/eye visual tracking with uncertain parameters, *IEEE Trans. on Robotics and Automation,* vol. 11, no. 5, pp. 725-732.

Pomares. J.; Chaumette. F. & Torres. F. (2007). Adaptive Visual Servoing by Simultaneous Camera Calibration, *Proc. of IEEE Int. Conf. on Robotics and Automation*, pp.2811-2816.

Ruf. A.; Tonko. M.; Horaud. R. & Nagel. H.-H. (1997) Visual tracking of an end effector by adaptive kinematic prediction, *Proc. of IEEE/RSJ Int. Conf. on Intelligent Robots and Systems,* pp. 893-898.

Shen. Y.; Song. D.; Liu. Y. H. & Li. K. (2003). Asymptotic trajectory tracking of manipulators using uncalibrated visual feedback," *IEEE/ASME Trans. on Mechatronics,* vo. 8, no. 1, pp. 87-98.

Slotine. J. J. & Li. W. (1987), On the adaptive control of robot manipulators, *Int. J. Robotics Research,* Vol. 6, pp. 49-59.

Wang H. & Liu. Y. H. (2006). Uncalibrated Visual Tracking Control without Visual Velocity, *Proc. of IEEE Int. Conf. on Robotics and Automation*, pp.2738-2743.

Wang. H. & Liu. Y. H. (2006). Uncalibrated Visual Tracking Control without Visual Velocity, *Proc. of IEEE Int. Conf. on Robotics and Automation*, pp.2738-2743.

Wang. H.; Liu. Y. H. & Zhou. D. (2007). Dynamic visual tracking for manipulators using an uncalibrated fxied camera, *IEEE Trans. on Robotics*, vol. 23, no. 3, pp. 610-617.

Yoshimi. B. H. & Allen. P. K. (1995). Alignment using an uncalibrated camera system, *IEEE.Trans. on Robotics and Automation*, vol. 11, no.4, pp. 516-521.

Robot Manipulators

Edited by Marco Ceccarelli

ISBN 978-953-7619-06-0

Hard cover, 546 pages

Publisher InTech

Published online 01, September, 2008

Published in print edition September, 2008

In this book we have grouped contributions in 28 chapters from several authors all around the world on the several aspects and challenges of research and applications of robots with the aim to show the recent advances and problems that still need to be considered for future improvements of robot success in worldwide frames. Each chapter addresses a specific area of modeling, design, and application of robots but with an eye to give an integrated view of what make a robot a unique modern system for many different uses and future potential applications. Main attention has been focused on design issues as thought challenging for improving capabilities and further possibilities of robots for new and old applications, as seen from today technologies and research programs. Thus, great attention has been addressed to control aspects that are strongly evolving also as function of the improvements in robot modeling, sensors, servo-power systems, and informatics. But even other aspects are considered as of fundamental challenge both in design and use of robots with improved performance and capabilities, like for example kinematic design, dynamics, vision integration.

InTech Europe

University Campus STeP Ri
Slavka Krautzeka 83/A
51000 Rijeka, Croatia
Phone: +385 (51) 770 447
Fax: +385 (51) 686 166
www.intechopen.com

InTech China

Unit 405, Office Block, Hotel Equatorial Shanghai
No.65, Yan An Road (West), Shanghai, 200040, China
中国上海市延安西路65号上海国际贵都大饭店办公楼405单元
Phone: +86-21-62489820
Fax: +86-21-62489821

IntechOpen